REPORT DOCUMENTATION PAGE

Form Approved
OMB No. 0704-0188

1. REPORT DATE
06 August 2018

2. REPORT TYPE
Briefing Charts

3. DATES COVERED *(From - To)*
21 July 2018 - 30 August 2018

4. TITLE AND SUBTITLE
Improved Models and Understanding for Field-Reversed Configuration (FRC) Thrusters (Briefing Charts)

5a. CONTRACT NUMBER

5b. GRANT NUMBER

5c. PROGRAM ELEMENT NUMBER

6. AUTHOR(S)
Robert Martin, Eder Sousa, Robert Lilly, Michael Kapper

5d. PROJECT NUMBER

5e. TASK NUMBER

5f. WORK UNIT NUMBER
Q200

7. PERFORMING ORGANIZATION NAME(S) AND ADDRESS(ES)
Air Force Research Laboratory (AFMC)
AFRL/RQRS
1 Ara Drive
Edwards AFB, CA 93524-7013

8. PERFORMING ORGANIZATION REPORT NUMBER

9. SPONSORING/MONITORING AGENCY NAME(S) AND ADDRESS(ES)

Air Force Research Laboratory (AFMC)
AFRL/RQR
5 Pollux Drive
Edwards AFB, CA 93524-7048

10. SPONSOR/MONITOR'S ACRONYM(S)

11. SPONSOR/MONITOR'S REPORT NUMBER(S)
AFRL-RQ-ED-VG-2018-259

12. DISTRIBUTION/AVAILABILITY STATEMENT
Distribution Statement A: Approved for Public Release; Distribution is Unlimited. PA Clearance Number: 18476 Clearance Date: 30 July 2018.

13. SUPPLEMENTARY NOTES
For presentation at AFOSR Space Propulsion and Power Annual Review; Arlington, Virginia, USA; August 7-10, 2018.
Prepared in collaboration with ERC, Inc.
The U.S. Government is joint author of the work and has the right to use, modify, reproduce, release, perform, display, or disclose the work.

14. ABSTRACT
Viewgraph/Briefing Charts

15. SUBJECT TERMS
N/A

16. SECURITY CLASSIFICATION OF:			17. LIMITATION OF ABSTRACT	18. NUMBER OF PAGES	19a. NAME OF RESPONSIBLE PERSON
a. REPORT	b. ABSTRACT	c. THIS PAGE			Robert Martin
					19b. TELEPHONE NUMBER *(Include area code)*
Unclassified	Unclassified	Unclassified	SAR	79	N/A

THE AIR FORCE RESEARCH LABORATORY
LEAD | DISCOVER | DEVELOP | DELIVER

IMPROVED MODELS AND UNDERSTANDING FOR FIELD-REVERSED CONFIGURATION (FRC) THRUSTERS

Robert Martin[1], Eder Sousa[2], Robert Lilly[2], Michael Kapper[2]

[1]AIR FORCE RESEARCH LABORATORY,
[2]ERC INC.,
EDWARDS AIR FORCE BASE, CA USA

AFOSR Space Propulsion and Power Review, 2018
Distribution A - Approved for public release;
Distribution unlimited.
PA clearance No. 18476

U.S. AIR FORCE

Outline

Field-Reversed Configuration:

- Concept from Fusion Energy
  - Challenge Scaling Down for Propulsion

RP3X FRC Thruster

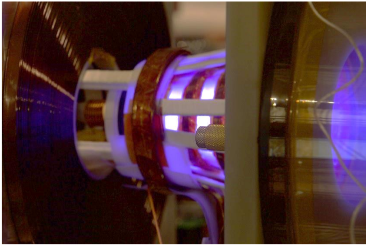

Field-Reversed Configuration:

- Concept from Fusion Energy
  - Challenge Scaling Down for Propulsion
- Electrodeless (+ Limits Erosion)

RP3X FRC Thruster

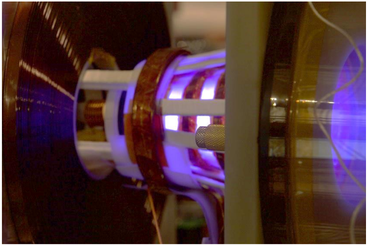

Field-Reversed Configuration:

- Concept from Fusion Energy
  - Challenge Scaling Down for Propulsion
- Electrodeless (+ Limits Erosion)
- Acceleration Mechanism $J \times B$
  + Enables Flexible Fuels

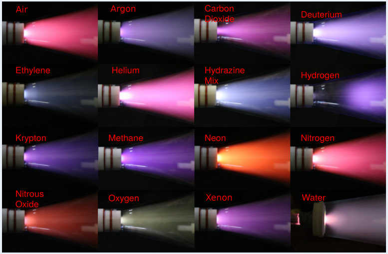

Pancotti, et al, “Adaptive Electric Propulsion for ISRU Missions”, 20th Adv. Space Prop., 11/2014

RP3X FRC Thruster

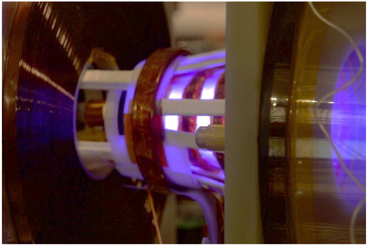

Field-Reversed Configuration:

- Concept from Fusion Energy
  - Challenge Scaling Down for Propulsion
- Electrodeless (+ Limits Erosion)
- Acceleration Mechanism $J \times B$
  + Enables Flexible Fuels
- Pulsed Operation
  +Tunable Thrust/ISP
  - Complex Coupled Dynamics
  - High Dimensional Parameter Space

RP3X FRC Thruster

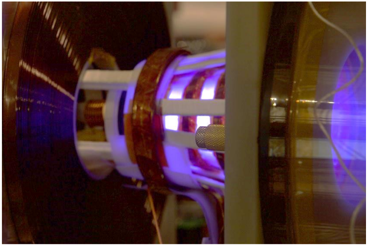

Field-Reversed Configuration:

- Concept from Fusion Energy
  - Challenge Scaling Down for Propulsion
- Electrodeless (+ Limits Erosion)
- Acceleration Mechanism $J \times B$
  + Enables Flexible Fuels
- Pulsed Operation
  +Tunable Thrust/ISP
  - Complex Coupled Dynamics
  - High Dimensional Parameter Space
- Common Challenges/Benefits for EM
  + MPD/PIT/PPT

Complex Devices to Design

RP3X FRC Thruster

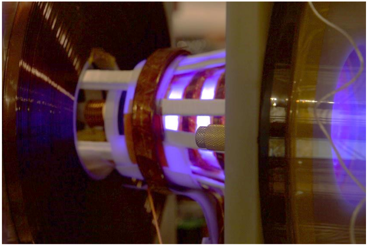

Field-Reversed Configuration:

- Concept from Fusion Energy
  - Challenge Scaling Down for Propulsion
- Electrodeless (+ Limits Erosion)
- Acceleration Mechanism $J \times B$
  + Enables Flexible Fuels
- Pulsed Operation
  +Tunable Thrust/ISP
  - Complex Coupled Dynamics
  - High Dimensional Parameter Space
- Common Challenges/Benefits for EM
  + MPD/PIT/PPT
  + Similar Tools Required

Complex Devices to Design
Pose Significant Modeling Challenge

RP3X FRC Thruster

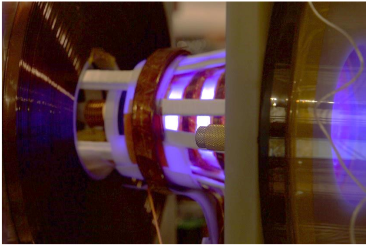

The Boltzmann Equation for $f(\mathbf{x}, \mathbf{v}; t)$:

$$\frac{\partial f_s}{\partial t} + \mathbf{v} \cdot \frac{\partial f_s}{\partial \mathbf{x}} + \frac{q_s}{m_s} (\mathbf{E} + \mathbf{v} \times \mathbf{B}) \frac{\partial f_s}{\partial \mathbf{v}} = \left(\frac{\partial f_s}{\partial t} \right)_{coll}$$

Range of Validity

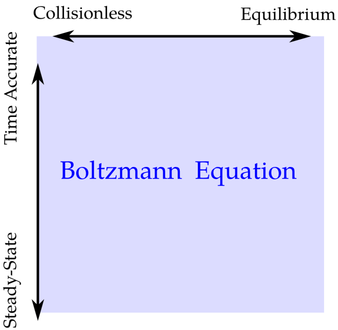

The Boltzmann Equation for $f(\mathbf{x}, \mathbf{v}; t)$:

$$\frac{\partial f_s}{\partial t} + \mathbf{v} \cdot \frac{\partial f_s}{\partial \mathbf{x}} + \frac{q_s}{m_s}(\mathbf{E} + \mathbf{v} \times \mathbf{B}) \frac{\partial f_s}{\partial \mathbf{v}} = \left(\frac{\partial f_s}{\partial t}\right)_{coll}$$

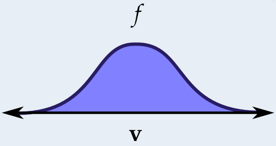

Range of Validity

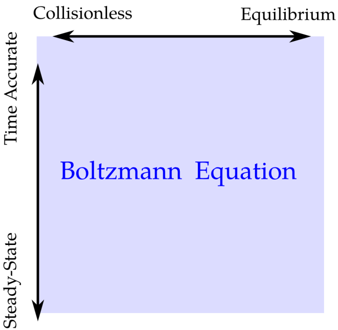

The Boltzmann Equation for $f(\mathbf{x}, \mathbf{v}; t)$:

$$\frac{\partial f_s}{\partial t} + \mathbf{v} \cdot \frac{\partial f_s}{\partial \mathbf{x}} + \frac{q_s}{m_s}(\mathbf{E} + \mathbf{v} \times \mathbf{B}) \frac{\partial f_s}{\partial \mathbf{v}} = \left(\frac{\partial f_s}{\partial t}\right)_{coll}$$

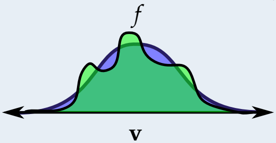

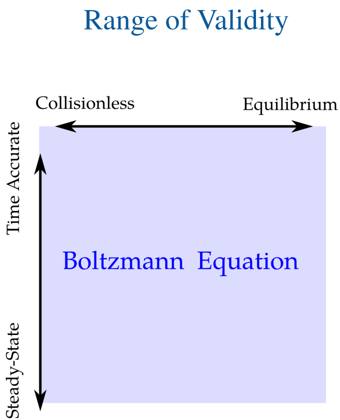

The Boltzmann Equation for $f(\mathbf{x}, \mathbf{v}; t)$:

$$\frac{\partial f_s}{\partial t} + \mathbf{v} \cdot \frac{\partial f_s}{\partial \mathbf{x}} + \frac{q_s}{m_s}(\mathbf{E} + \mathbf{v} \times \mathbf{B}) \frac{\partial f_s}{\partial \mathbf{v}} = \left(\frac{\partial f_s}{\partial t}\right)_{coll}$$

- Collisionality Limits:

$$\text{(Vlasov) } 0 \leftarrow \left(\frac{\partial f_s}{\partial t}\right)_{coll} \rightarrow \infty \text{ (Euler)}$$

Range of Validity

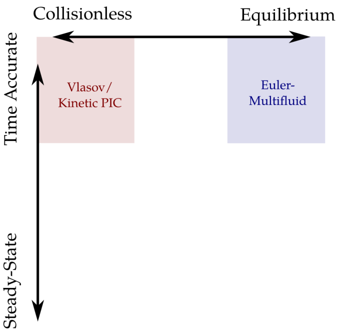

The Boltzmann Equation for $f(\mathbf{x}, \mathbf{v}; t)$:

$$\frac{\partial f_s}{\partial t} + \mathbf{v} \cdot \frac{\partial f_s}{\partial \mathbf{x}} + \frac{q_s}{m_s}(\mathbf{E} + \mathbf{v} \times \mathbf{B}) \frac{\partial f_s}{\partial \mathbf{v}} = \left(\frac{\partial f_s}{\partial t}\right)_{coll}$$

- Collisionality Limits:
  $$\text{(Vlasov) } 0 \leftarrow \left(\frac{\partial f_s}{\partial t}\right)_{coll} \rightarrow \infty \text{ (Euler)}$$
- Ohm's Law:
  $$(m_e \ll m_i) \rightarrow \frac{\partial f_e}{\partial t} \equiv 0$$

Range of Validity

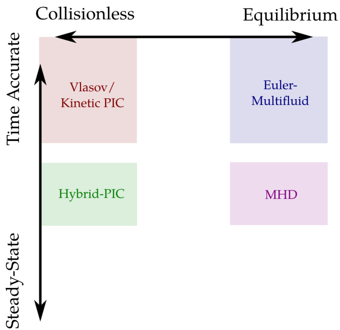

The Boltzmann Equation for $f(\mathbf{x}, \mathbf{v}; t)$:

$$\frac{\partial f_s}{\partial t} + \mathbf{v} \cdot \frac{\partial f_s}{\partial \mathbf{x}} + \frac{q_s}{m_s}(\mathbf{E} + \mathbf{v} \times \mathbf{B}) \frac{\partial f_s}{\partial \mathbf{v}} = \left(\frac{\partial f_s}{\partial t}\right)_{coll}$$

- Collisionality Limits:
  (Vlasov) $0 \leftarrow \left(\frac{\partial f_s}{\partial t}\right)_{coll} \rightarrow \infty$ (Euler)
- Ohm's Law:
  $(m_e \ll m_i) \rightarrow \frac{\partial f_e}{\partial t} \equiv 0$
- Steady-State Solutions:
  $\frac{\partial}{\partial t} \equiv 0$

Range of Validity

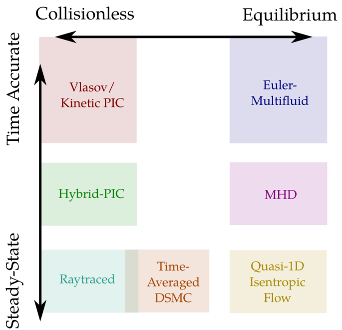

The Boltzmann Equation for $f(\mathbf{x}, \mathbf{v}; t)$:

$$\frac{\partial f_s}{\partial t} + \mathbf{v} \cdot \frac{\partial f_s}{\partial \mathbf{x}} + \frac{q_s}{m_s}(\mathbf{E} + \mathbf{v} \times \mathbf{B}) \frac{\partial f_s}{\partial \mathbf{v}} = \left(\frac{\partial f_s}{\partial t}\right)_{coll}$$

- Collisionality Limits:
  (Vlasov) $0 \leftarrow \left(\frac{\partial f_s}{\partial t}\right)_{coll} \rightarrow \infty$ (Euler)
- Ohm's Law:
  $(m_e \ll m_i) \rightarrow \frac{\partial f_e}{\partial t} \equiv 0$
- Steady-State Solutions:
  $\frac{\partial}{\partial t} \equiv 0$

Limits Exchange Accuracy for Cost

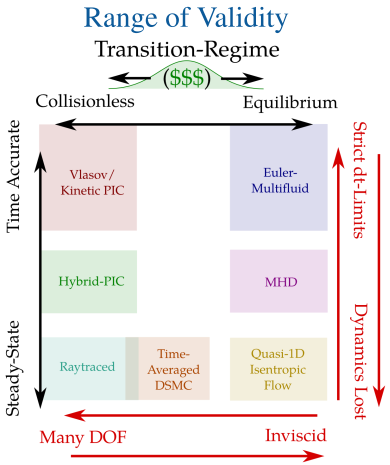

The Boltzmann Equation for $f(\mathbf{x}, \mathbf{v}; t)$:

$$\frac{\partial f_s}{\partial t} + \mathbf{v} \cdot \frac{\partial f_s}{\partial \mathbf{x}} + \frac{q_s}{m_s}(\mathbf{E} + \mathbf{v} \times \mathbf{B}) \frac{\partial f_s}{\partial \mathbf{v}} = \left(\frac{\partial f_s}{\partial t}\right)_{coll}$$

- Collisionality Limits:
  $$\text{(Vlasov) } 0 \leftarrow \left(\frac{\partial f_s}{\partial t}\right)_{coll} \rightarrow \infty \text{ (Euler)}$$
- Ohm's Law:
  $$(m_e \ll m_i) \rightarrow \frac{\partial f_e}{\partial t} \equiv 0$$
- Steady-State Solutions:
  $$\frac{\partial}{\partial t} \equiv 0$$

Limits Exchange Accuracy for Cost

Transition Incurs Costs to Limit

Range of Validity

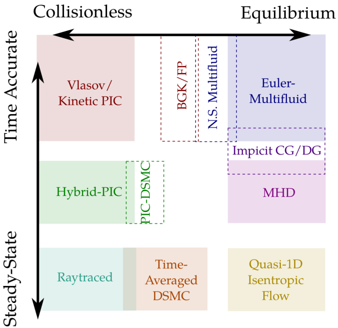

Tool Development Spanning Regimes

The Boltzmann Equation for $f(\mathbf{x}, \mathbf{v}; t)$:

$$\frac{\partial f_s}{\partial t} + \mathbf{v} \cdot \frac{\partial f_s}{\partial \mathbf{x}} + \frac{q_s}{m_s} (\mathbf{E} + \mathbf{v} \times \mathbf{B}) \frac{\partial f_s}{\partial \mathbf{v}} = \left(\frac{\partial f_s}{\partial t} \right)_{coll}$$

- Collisionality Limits:
  (Vlasov) $0 \leftarrow \left(\frac{\partial f_s}{\partial t} \right)_{coll} \rightarrow \infty$ (Euler)
- Ohm's Law:
  $(m_e \ll m_i) \rightarrow \frac{\partial f_e}{\partial t} \equiv 0$
- Steady-State Solutions:
  $\frac{\partial}{\partial t} \equiv 0$

Limits Exchange Accuracy for Cost
Transition Incurs Costs to Limit
$(\nu = 0 \neq \nu \rightarrow 0)$
But Relaxes/Removes Assumptions

Range of Validity

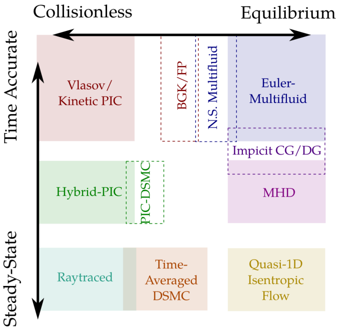

The Boltzmann Equation for $f(\mathbf{x}, \mathbf{v}; t)$:

$$\frac{\partial f_s}{\partial t} + \mathbf{v} \cdot \frac{\partial f_s}{\partial \mathbf{x}} + \frac{q_s}{m_s}(\mathbf{E} + \mathbf{v} \times \mathbf{B}) \frac{\partial f_s}{\partial \mathbf{v}} = \left(\frac{\partial f_s}{\partial t}\right)_{coll}$$

- Collisionality Limits:
  $$(\text{Vlasov})\ 0 \leftarrow \left(\frac{\partial f_s}{\partial t}\right)_{coll} \rightarrow \infty\ (\text{Euler})$$
- Ohm's Law:
  $$(m_e \ll m_i) \rightarrow \frac{\partial f_e}{\partial t} \equiv 0$$
- Steady-State Solutions:
  $$\frac{\partial}{\partial t} \equiv 0$$

Limits Exchange Accuracy for Cost
Transition Incurs Costs to Limit

TURF: For Exploring Efficient Methods
Minimizing Cost/Accuracy & Redundancy

Range of Validity

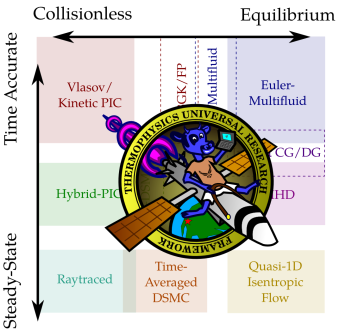

Progress on MF Formation/Reversal

Apollo Formation Simulations:

- RMF $\rightarrow j_\theta \rightarrow B_z$-Reversal

DG FRC-Formation

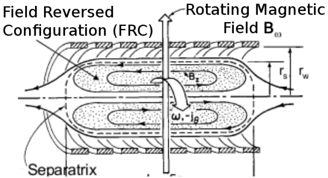

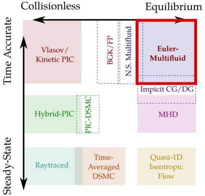

Apollo Formation Simulations:

- RMF $\rightarrow j_\theta \rightarrow B_z$-Reversal
- Initially Conditions:
  Fully Ionized Xe Gas
  $n_i = n_e = 10^{20}/m^3$
  60G Bias (Z) + 60G RMF @ 1MHz

DG FRC-Formation

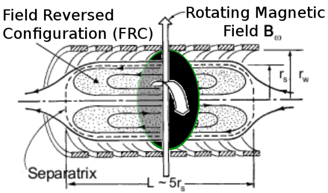

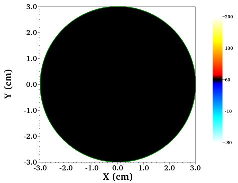

$t = 0\omega$

Apollo Formation Simulations:

- RMF $\rightarrow j_\theta \rightarrow B_z$-Reversal
- Initially Conditions:
  Fully Ionized Xe Gas
  $n_i = n_e = 10^{20}/m^3$
  60G Bias (Z) + 60G RMF @ 1MHz
- Strong Reversal B_z Reversal by 180°

DG FRC-Formation

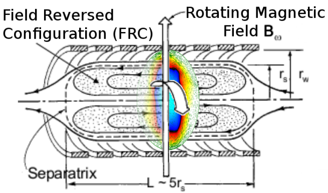

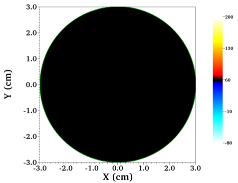

t=0-0.5ω

Apollo Formation Simulations:

- RMF $\rightarrow j_\theta \rightarrow B_z$-Reversal
- Initially Conditions:
  Fully Ionized Xe Gas
  $n_i = n_e = 10^{20}/m^3$
  60G Bias (Z) + 60G RMF @ 1MHz
- Strong Reversal B_z Reversal by 180°
- Reversal Weakens, 180°-360°

DG FRC-Formation

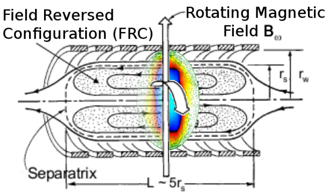

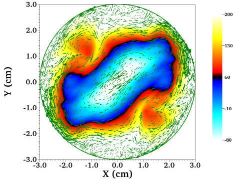

t=0.5-1.0ω

Apollo Formation Simulations:

- RMF $\rightarrow j_\theta \rightarrow B_z$-Reversal
- Initially Conditions:
  Fully Ionized Xe Gas
  $n_i = n_e = 10^{20}/m^3$
  60G Bias (Z) + 60G RMF @ 1MHz
- Strong Reversal B_z Reversal by 180°
- Reversal Weakens, 180°-360°
- Cycle Repeats
  (But Lower Amplitude)

DG FRC-Formation

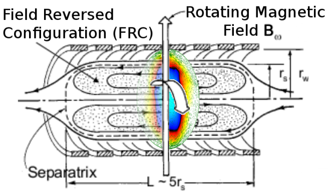

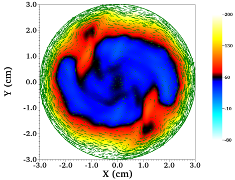

t=1.0-2.0ω

Apollo Formation Simulations:

- RMF $\to j_\theta \to B_z$-Reversal
- Initially Conditions:
  Fully Ionized Xe Gas
  $n_i = n_e = 10^{20}/m^3$
  60G Bias (Z) + 60G RMF @ 1MHz
- Strong Reversal B_z Reversal by 180°
- Reversal Weakens, 180°-360°
- Cycle Repeats
  (But Lower Amplitude)
- Parameter Space is being Explored

DG FRC-Formation

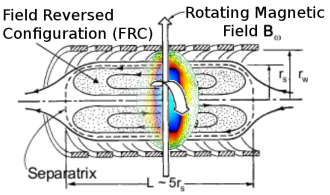

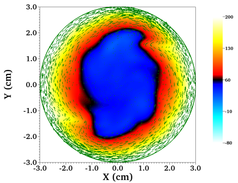

$t = 1.0\text{-}2.0\omega$

Apollo Formation Simulations:

- RMF $\rightarrow j_\theta \rightarrow B_z$-Reversal
- Initially Conditions:
  Fully Ionized Xe Gas
  $n_i = n_e = 10^{20}/m^3$
  60G Bias (Z) + 60G RMF @ 1MHz
- Strong Reversal B_z Reversal by 180°
- Reversal Weakens, 180°-360°
- Cycle Repeats
  (But Lower Amplitude)
- Parameter Space is being Explored

Also Needs Experimental Validation!

DG FRC-Formation

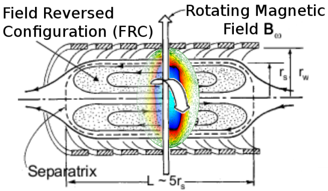

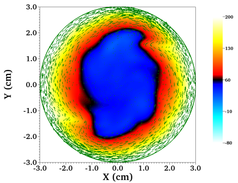

$t = 1.0\text{-}2.0\omega$

High Fidelity Validation:

- FRCs are Dynamic Pulsed Devices

DG FRC-Formation

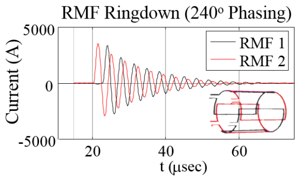

MSNW Ar FRC Formation

High Fidelity Validation:

- FRCs are Dynamic Pulsed Devices
- Ext. Probes Probes avoid Disruption
  ...but Mostly Limited View

DG FRC-Formation

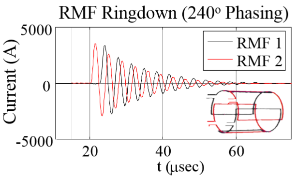

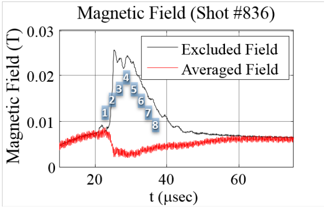

MSNW Ar FRC Formation

High Fidelity Validation:

- FRCs are Dynamic Pulsed Devices
- Ext. Probes Probes avoid Disruption
  ...but Mostly Limited View
- Fast Camera:
  Absolute Magnitudes Difficult
  Relatively High Dimensional

DG FRC-Formation

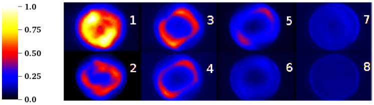

(False Color Intensity - MSNW Fast Camera Studies)

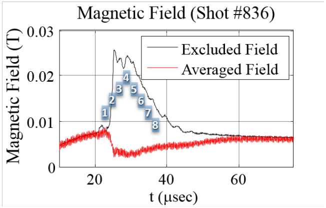

MSNW Ar FRC Formation

High Fidelity Validation:

- FRCs are Dynamic Pulsed Devices
- Ext. Probes Probes avoid Disruption
  ...but Mostly Limited View
- Fast Camera:
  Absolute Magnitudes Difficult
  Relatively High Dimensional
- Emission from IonMix (n_e,T_e) Table
- Plotted at Equivalent ω

DG FRC-Formation

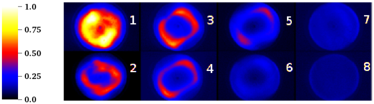

(False Color Intensity - MSNW Fast Camera Studies)

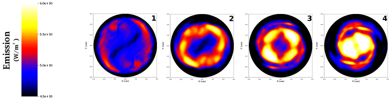

(Apollo Multifluid Simulation Emission Intensity)

RADIATIVE EMISSION VALIDATION

High Fidelity Validation:

- FRCs are Dynamic Pulsed Devices
- Ext. Probes Probes avoid Disruption
  ...but Mostly Limited View
- Fast Camera:
  Absolute Magnitudes Difficult
  Relatively High Dimensional
- Emission from IonMix (n_e, T_e) Table
- Plotted at Equivalent ω
- Similar Structures in **2** & **3**
  Despite Different Conditions

DG FRC-Formation

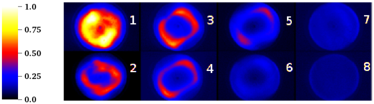

(False Color Intensity - MSNW Fast Camera Studies)

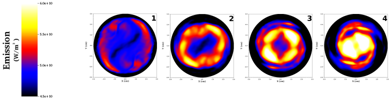

(Apollo Multifluid Simulation Emission Intensity)

High Fidelity Validation:

- FRCs are Dynamic Pulsed Devices
- Ext. Probes Probes avoid Disruption
  ...but Mostly Limited View
- Fast Camera:
  Absolute Magnitudes Difficult
  Relatively High Dimensional
- Emission from IonMix (n_e, T_e) Table
- Plotted at Equivalent ω
- Similar Structures in **2** & **3**
  Despite Different Conditions
- Experiment Relaxes but
  Simulation Intensifies in **4+**

DG FRC-Formation

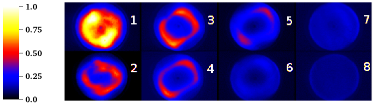

(False Color Intensity - MSNW Fast Camera Studies)

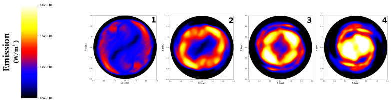

(Apollo Multifluid Simulation Emission Intensity)

High Fidelity Validation:

- FRCs are Dynamic Pulsed Devices
- Ext. Probes Probes avoid Disruption
  ...but Mostly Limited View
- Fast Camera:
  Absolute Magnitudes Difficult
  Relatively High Dimensional
- Emission from IonMix (n_e, T_e) Table
- Plotted at Equivalent ω
- Similar Structures in **2** & **3**
  Despite Different Conditions
- Experiment Relaxes but
  Simulation Intensifies in **4+**

Model Needs Additional Physics

DG FRC-Formation

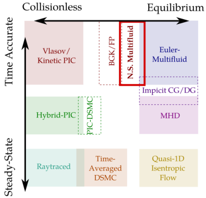

+Circuit Model
+CR-Model

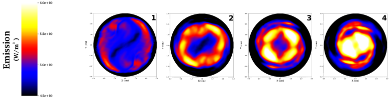

(Apollo Multifluid Simulation Emission Intensity)

AFRL Model Development/Project Synergies:

Model	Need	Platform	Project	Progress	Demo
Circuit	BC/Energy Cons.	TURF	1 & 2	Runtime Arbitrary ODE B.C.s	Lorenz DSMC Inflow
Radiative	Physics/Energy Cons.	R&D	3	Full Level-Grouped Ar Model	Abrantes PhD (UCLA 2018)
Multi-Fluid	Physics/Stability	Apollo	4	N.S./Braginskii	Poiselle/Taylor Couette
Multi-Fluid	Physics/Stability	TURF/R&D	4	Hybrid Entropy/Energy Cons.	Einfeldt/Step/Cylinder/Jet
Kinetic	Charge Separation	TURF	1 & 4	Boltzmann-n_e vs. $\langle n_e \rangle$	Quasi-1D HET

Projects:

1. In-House AFRL 6.2 Research
2. AFOSR Comp Math Lab-Task (New), PO: Fahroo
3. AFOSR Plasma/Electro-energetics Lab-Task, PO: Marshall
4. AFOSR Space Propulsion & Power, PO: Birkan

AFRL Model Development/Project Synergies:

Model	Need	Platform	Project	Progress	Demo
Circuit	BC/Energy Cons.	TURF	1 & 2	Runtime Arbitrary ODE B.C.s	Lorenz DSMC Inflow
Radiative	Physics/Energy Cons.	R&D	3	Full Level-Grouped Ar Model	Abrantes PhD (UCLA 2018)
Multi-Fluid	Physics/Stability	Apollo	4	N.S./Braginskii	Poiselle/Taylor Couette
Multi-Fluid	Physics/Stability	TURF/R&D	4	Hybrid Entropy/Energy Cons.	Einfeldt/Step/Cylinder/Jet
Kinetic	Charge Separation	TURF	1 & 4	Boltzmann-n_e vs. $\langle n_e \rangle$	Quasi-1D HET

Projects:

1. In-House AFRL 6.2 Research
2. AFOSR Comp Math Lab-Task (New), PO: Fahroo
3. AFOSR Plasma/Electro-energetics Lab-Task, PO: Marshall
4. AFOSR Space Propulsion & Power, PO: Birkan

$$\partial_t \mathbf{Q} + \nabla \cdot \mathbf{F}^{Hyp} + \nabla \cdot \mathbf{F}^{Para} = \mathbf{S}^{EM} + \mathbf{S}^{ie}$$

$$\begin{array}{ccccc}
\mathbf{Q} & \mathbf{F}^{Hyp} & \mathbf{F}^{Para} & \mathbf{S}^{EM} & \mathbf{S}^{ie} \\
\begin{bmatrix} \rho_e \\ \rho_e \mathbf{u_e} \\ \mathscr{E}_e \\ \rho_i \\ \rho_i \mathbf{u_i} \\ \mathscr{E}_i \end{bmatrix} &
\begin{bmatrix} \rho_e \mathbf{u_e} \\ \rho_e \mathbf{u_e} \mathbf{u_e} + p_e \mathbf{I} \\ \mathbf{u_e} \cdot (\mathscr{E}_e + p_e) \mathbf{I} \\ \rho_i \mathbf{u_i} \\ \rho_i \mathbf{u_i} \mathbf{u_i} + p_i \mathbf{I} \\ \mathbf{u_i} \cdot (\mathscr{E}_i + p_i) \mathbf{I} \end{bmatrix} &
\begin{bmatrix} 0 \\ \mathbf{\Pi}_e \\ \mathbf{u_e} \cdot \mathbf{\Pi}_e + \mathbf{q_e} \\ 0 \\ \mathbf{\Pi}_i \\ \mathbf{u_i} \cdot \mathbf{\Pi}_i + \mathbf{q_i} \end{bmatrix} &
\begin{bmatrix} 0 \\ q_e n_e (\mathbf{E} + \mathbf{u_e} \times \mathbf{B}) \\ q_e n_e \mathbf{u_e} \mathbf{E} \\ 0 \\ q_i n_i (\mathbf{E} + \mathbf{u_i} \times \mathbf{B}) \\ q_i n_i \mathbf{u_i} \mathbf{E} \end{bmatrix} &
\begin{bmatrix} 0 \\ -\mathbf{R}_{ie} \\ \mathbf{u}_e \cdot \mathbf{R}_{ie} + \mathbf{Q}_{ie}^e \\ 0 \\ -\mathbf{R}_{ei} \\ \mathbf{u}_i \cdot \mathbf{R}_{ei} + \mathbf{Q}_{ei}^i \end{bmatrix}
\end{array}$$

The EOS used here: $p = nk_B T$. Energy $\mathscr{E} = \frac{p}{\gamma - 1} + \frac{1}{2}\rho \mathbf{u} \cdot \mathbf{u}$.

$$\partial_t \mathbf{Q} + \nabla \cdot \mathbf{F}^{Hyp} + \nabla \cdot \mathbf{F}^{Para} = \mathbf{S}^{EM} + \mathbf{S}^{ie}$$

$$\begin{array}{ccccc}
\mathbf{Q} & \mathbf{F}^{Hyp} & \mathbf{F}^{Para} & \mathbf{S}^{EM} & \mathbf{S}^{ie} \\
\begin{bmatrix} \rho_e \\ \rho_e \mathbf{u_e} \\ \mathcal{E}_e \\ \rho_i \\ \rho_i \mathbf{u_i} \\ \mathcal{E}_i \end{bmatrix} &
\begin{bmatrix} \rho_e \mathbf{u_e} \\ \rho_e \mathbf{u_e} \mathbf{u_e} + p_e \mathbf{I} \\ \mathbf{u_e} \cdot (\mathcal{E}_e + p_e) \mathbf{I} \\ \rho_i \mathbf{u_i} \\ \rho_i \mathbf{u_i} \mathbf{u_i} + p_i \mathbf{I} \\ \mathbf{u_i} \cdot (\mathcal{E}_i + p_i) \mathbf{I} \end{bmatrix} &
\begin{bmatrix} 0 \\ \mathbf{\Pi}_e \\ \mathbf{u_e} \cdot \mathbf{\Pi}_e + \mathbf{q_e} \\ 0 \\ \mathbf{\Pi}_i \\ \mathbf{u_i} \cdot \mathbf{\Pi}_i + \mathbf{q_i} \end{bmatrix} &
\begin{bmatrix} 0 \\ q_e n_e (\mathbf{E} + \mathbf{u_e} \times \mathbf{B}) \\ q_e n_e \mathbf{u_e} \mathbf{E} \\ 0 \\ q_i n_i (\mathbf{E} + \mathbf{u_i} \times \mathbf{B}) \\ q_i n_i \mathbf{u_i} \mathbf{E} \end{bmatrix} &
\begin{bmatrix} 0 \\ -\mathbf{R}_{ie} \\ \mathbf{u}_e \cdot \mathbf{R}_{ie} + \mathbf{Q}_{ie}^e \\ 0 \\ -\mathbf{R}_{ei} \\ \mathbf{u}_i \cdot \mathbf{R}_{ei} + \mathbf{Q}_{ei}^i \end{bmatrix}
\end{array}$$

The EOS used here: $p = nk_B T$. Energy $\mathcal{E} = \frac{p}{\gamma - 1} + \frac{1}{2}\rho \mathbf{u} \cdot \mathbf{u}$.

$$\partial_t \mathbf{Q} + \nabla \cdot \mathbf{F}^{Hyp} + \nabla \cdot \mathbf{F}^{Para} = \mathbf{S}^{EM} + \mathbf{S}^{ie}$$

$$\begin{array}{ccccc}
\mathbf{Q} & \mathbf{F}^{Hyp} & \mathbf{F}^{Para} & \mathbf{S}^{EM} & \mathbf{S}^{ie} \\
\begin{bmatrix} \rho_e \\ \rho_e \mathbf{u_e} \\ \mathscr{E}_e \\ \rho_i \\ \rho_i \mathbf{u_i} \\ \mathscr{E}_i \end{bmatrix} &
\begin{bmatrix} \rho_e \mathbf{u_e} \\ \rho_e \mathbf{u_e} \mathbf{u_e} + p_e \mathbf{I} \\ \mathbf{u_e} \cdot (\mathscr{E}_e + p_e) \mathbf{I} \\ \rho_i \mathbf{u_i} \\ \rho_i \mathbf{u_i} \mathbf{u_i} + p_i \mathbf{I} \\ \mathbf{u_i} \cdot (\mathscr{E}_i + p_i) \mathbf{I} \end{bmatrix} &
\begin{bmatrix} 0 \\ \mathbf{\Pi}_e \\ \mathbf{u_e} \cdot \mathbf{\Pi}_e + \mathbf{q_e} \\ 0 \\ \mathbf{\Pi}_i \\ \mathbf{u_i} \cdot \mathbf{\Pi}_i + \mathbf{q_i} \end{bmatrix} &
\begin{bmatrix} 0 \\ q_e n_e (\mathbf{E} + \mathbf{u_e} \times \mathbf{B}) \\ q_e n_e \mathbf{u_e} \mathbf{E} \\ 0 \\ q_i n_i (\mathbf{E} + \mathbf{u_i} \times \mathbf{B}) \\ q_i n_i \mathbf{u_i} \mathbf{E} \end{bmatrix} &
\begin{bmatrix} 0 \\ -\mathbf{R}_{ie} \\ \mathbf{u}_e \cdot \mathbf{R}_{ie} + \mathbf{Q}^e_{ie} \\ 0 \\ -\mathbf{R}_{ei} \\ \mathbf{u}_i \cdot \mathbf{R}_{ei} + \mathbf{Q}^i_{ei} \end{bmatrix}
\end{array}$$

The EOS used here: $p = nk_BT$. Energy $\mathscr{E} = \frac{p}{\gamma - 1} + \frac{1}{2}\rho \mathbf{u} \cdot \mathbf{u}$.

Progress:

Classic (Newtonian) and Braginskii Formulations Implemented

$$\partial_t \mathbf{Q} + \nabla \cdot \mathbf{F}^{Hyp} + \nabla \cdot \mathbf{F}^{Para} = \mathbf{S}^{EM} + \mathbf{S}^{ie}$$

$$\begin{array}{ccccc} \mathbf{Q} & \mathbf{F}^{Hyp} & \mathbf{F}^{Para} & \mathbf{S}^{EM} & \mathbf{S}^{ie} \\ \begin{bmatrix} \rho_e \\ \rho_e \mathbf{u_e} \\ \mathscr{E}_e \\ \rho_i \\ \rho_i \mathbf{u_i} \\ \mathscr{E}_i \end{bmatrix} & \begin{bmatrix} \rho_e \mathbf{u_e} \\ \rho_e \mathbf{u_e} \mathbf{u_e} + p_e \mathbf{I} \\ \mathbf{u_e} \cdot (\mathscr{E}_e + p_e) \mathbf{I} \\ \rho_i \mathbf{u_i} \\ \rho_i \mathbf{u_i} \mathbf{u_i} + p_i \mathbf{I} \\ \mathbf{u_i} \cdot (\mathscr{E}_i + p_i) \mathbf{I} \end{bmatrix} & \begin{bmatrix} 0 \\ \mathbf{\Pi}_e \\ \mathbf{u_e} \cdot \mathbf{\Pi}_e + \mathbf{q_e} \\ 0 \\ \mathbf{\Pi}_i \\ \mathbf{u_i} \cdot \mathbf{\Pi}_i + \mathbf{q_i} \end{bmatrix} & \begin{bmatrix} 0 \\ q_e n_e (\mathbf{E} + \mathbf{u_e} \times \mathbf{B}) \\ q_e n_e \mathbf{u_e} \mathbf{E} \\ 0 \\ q_i n_i (\mathbf{E} + \mathbf{u_i} \times \mathbf{B}) \\ q_i n_i \mathbf{u_i} \mathbf{E} \end{bmatrix} & \begin{bmatrix} 0 \\ -\mathbf{R}_{ie} \\ \mathbf{u}_e \cdot \mathbf{R}_{ie} + \mathbf{Q}^e_{ie} \\ 0 \\ -\mathbf{R}_{ei} \\ \mathbf{u}_i \cdot \mathbf{R}_{ei} + \mathbf{Q}^i_{ei} \end{bmatrix} \end{array}$$

The EOS used here: $p = nk_B T$. Energy $\mathscr{E} = \frac{p}{\gamma - 1} + \frac{1}{2}\rho \mathbf{u} \cdot \mathbf{u}$.

Progress:

Classic (Newtonian) and Braginskii Formulations Implemented

Validation Cases:

Newtonian	Braginskii
Channel Flow: ✓	Hartman: (Pending)
Cylindrical Couette: ✓	Magneto-Rotational Instability: (Pending)

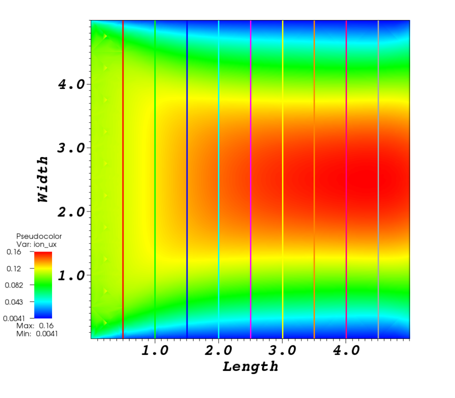

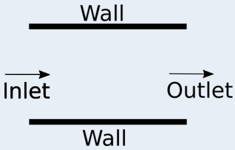

- A solid, no slip, boundary is enforced at the walls
- The input boundary uses a fixed Dirichlet condition. The flow is low subsonic (0.10 Mach).
- The exit using a von Neumann boundary condition on all variables except for pressure, which is set to the inlet condition.
- The chosen Reynolds number is approximately 30.

Channel Flow Results

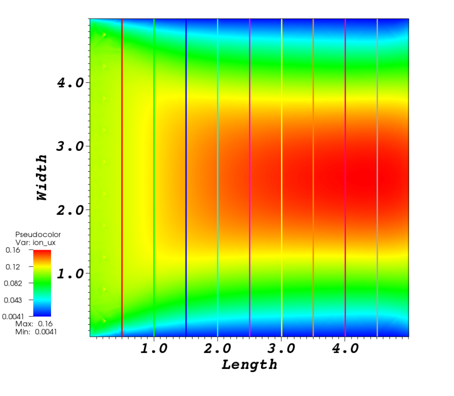

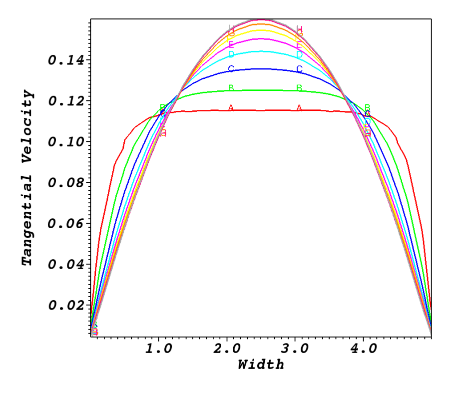

- A solid, no slip, boundary is enforced at the walls
- The input boundary uses a fixed Dirichlet condition. The flow is low subsonic (0.10 Mach).
- The exit using a von Neumann boundary condition on all variables except for pressure, which is set to the inlet condition.
- The chosen Reynolds number is approximately 30.

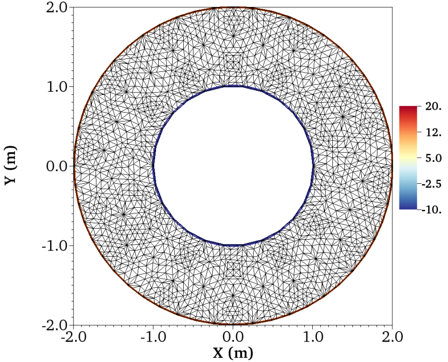

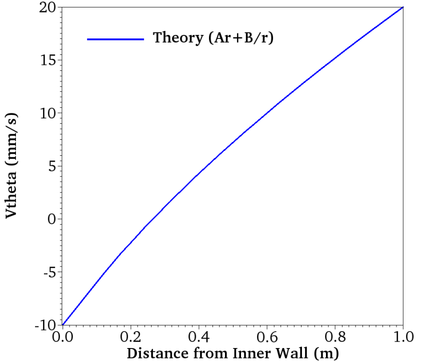

- Counter rotating solid, no slip, boundary is enforced at the inner/outer walls
- Reynolds number independent solution is rapidly established
- Good Agreement with Analytic Solution Attained

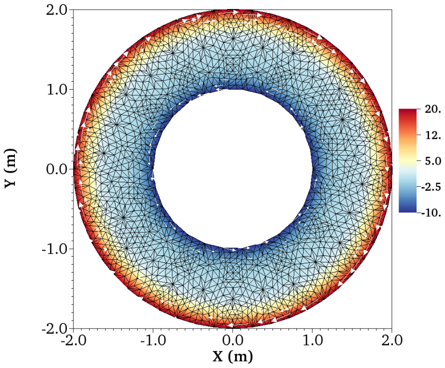

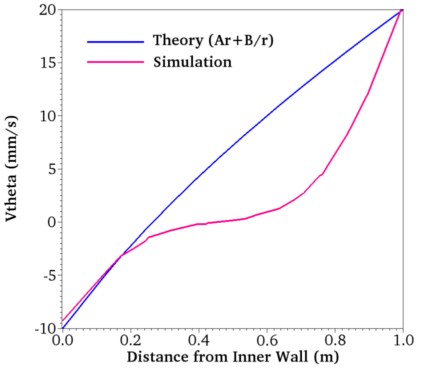

- Counter rotating solid, no slip, boundary is enforced at the inner/outer walls
- Reynolds number independent solution is rapidly established
- Good Agreement with Analytic Solution Attained

Entropy Formulation:

- Strong Rarefactions often break Fluid Codes (i.e. Negative Pressures/Artificial Heating)
- Low-β Numerical Instabilities in Apollo (Low-T_e)

Einfeldt 1-2-3 : Energy

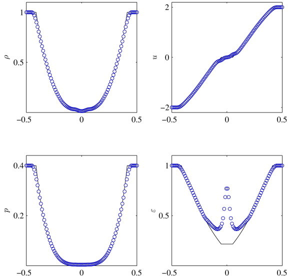

Solution to Einfeldt's 1-2-3 problem as obtained with conservation of energy. (Kapper PhD, OSU, '09)

Entropy Conservation and Hybridization

Entropy Formulation:

- Strong Rarefactions often break Fluid Codes (i.e. Negative Pressures/Artificial Heating)
- Low-β Numerical Instabilities in Apollo (Low-T_e)
- Low-Power Lab Experiments are Low-T_e ($\approx$10eV)
- Relevant Regime Numerically Inaccessible (i.e. T_e<20eV)

Einfeldt 1-2-3 : Energy

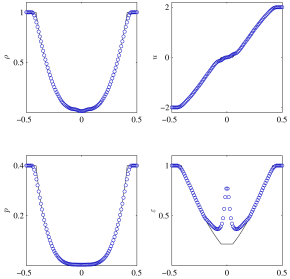

Solution to Einfeldt's 1-2-3 problem as obtained with conservation of energy. (Kapper PhD, OSU, '09)

Entropy Formulation:

- Strong Rarefactions often break Fluid Codes (i.e. Negative Pressures/Artificial Heating)
- Low-β Numerical Instabilities in Apollo (Low-T_e)
- Low-Power Lab Experiments are Low-T_e ($\approx$10eV)
- Relevant Regime Numerically Inaccessible (i.e. T_e<20eV)
- Entropy Cons. Helps for Strong Expansions (Ch.8, Kapper PhD, OSU '09)

Einfeldt 1-2-3 : Entropy

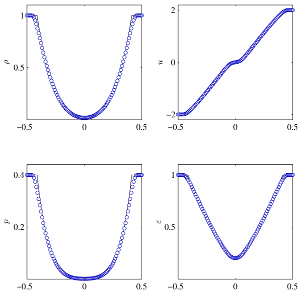

Solution to Einfeldt's 1-2-3 problem as obtained with conservation of entropy. (Kapper PhD, OSU, '09)

Entropy Formulation:

- Strong Rarefactions often break Fluid Codes (i.e. Negative Pressures/Artificial Heating)
- Low-β Numerical Instabilities in Apollo (Low-T_e)
- Low-Power Lab Experiments are Low-T_e ($\approx$10eV)
- Relevant Regime Numerically Inaccessible (i.e. T_e<20eV)
- Entropy Cons. Helps for Strong Expansions (Ch.8, Kapper PhD, OSU '09)
- Updated Method Enables Extreme Pressure Ratios (Kapper, 2018)

Einfeldt Vacuum Limit : Entropy

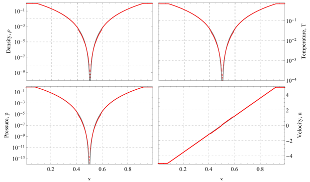

Solution to Einfeldt's Vacuum Limit (Mach 5, γ=7/5) problem as obtained with conservation of entropy and new linearization. (Kapper 18)

$$T/T_0=10^{-4}$$
$$\rho/\rho_0=10^{-9}$$
$$P/P_0=10^{-13}$$

Entropy Formulation:

- Strong Rarefactions often break Fluid Codes (i.e. Negative Pressures/Artificial Heating)
- Low-β Numerical Instabilities in Apollo (Low-T_e)
- Low-Power Lab Experiments are Low-T_e ($\approx$10eV)
- Relevant Regime Numerically Inaccessible (i.e. T_e<20eV)
- Entropy Cons. Helps for Strong Expansions (Ch.8, Kapper PhD, OSU '09)
- Updated Method Enables Extreme Pressure Ratios (Kapper, 2018)
- Apollo $Q \rightarrow$ Electron Entropy Cons. (Sousa, TBD)

$$\begin{array}{ccc} \mathbf{Q} & & \mathbf{Q} \\ \begin{bmatrix} \rho_e \\ \rho_e \mathbf{u_e} \\ \mathscr{E}_e \\ \rho_i \\ \rho_i \mathbf{u_i} \\ \mathscr{E}_i \end{bmatrix} & \rightarrow & \begin{bmatrix} \rho_e \\ \rho_e \mathbf{u_e} \\ \rho_e s_e \\ \rho_i \\ \rho_i \mathbf{u_i} \\ \mathscr{E}_i \end{bmatrix} \end{array}$$

$$s_e = P_e / \rho_e^{\gamma}$$

Entropy Formulation:

- Strong Rarefactions often break Fluid Codes (i.e. Negative Pressures/Artificial Heating)
- Low-β Numerical Instabilities in Apollo (Low-T_e)
- Low-Power Lab Experiments are Low-T_e ($\approx$10eV)
- Relevant Regime Numerically Inaccessible (i.e. T_e<20eV)
- Entropy Cons. Helps for Strong Expansions (Ch.8, Kapper PhD, OSU '09)
- Updated Method Enables Extreme Pressure Ratios (Kapper, 2018)
- Apollo $Q \rightarrow$ Electron Entropy Cons. (Sousa, TBD)
- Extending to Hybrid Energy/Entropy Cons. (Kapper, 2018)

Linde-Roe Corner Expansion

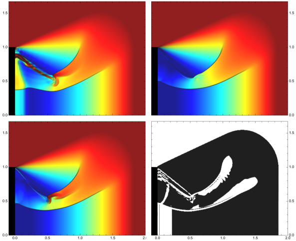

Top Left: Energy Conservation
Top Right: Entropy Conservation
Bottom Left: Hybrid Solution
Bottom Right: Hybrid Compression Flag

(Kapper '18)

Entropy Formulation:

- Strong Rarefactions often break Fluid Codes (i.e. Negative Pressures/Artificial Heating)
- Low-β Numerical Instabilities in Apollo (Low-T_e)
- Low-Power Lab Experiments are Low-T_e ($\approx$10eV)
- Relevant Regime Numerically Inaccessible (i.e. T_e<20eV)
- Entropy Cons. Helps for Strong Expansions (Ch.8, Kapper PhD, OSU '09)
- Updated Method Enables Extreme Pressure Ratios (Kapper, 2018)
- Apollo $Q \rightarrow$ Electron Entropy Cons. (Sousa, TBD)
- Extending to Hybrid Energy/Entropy Cons. (Kapper, 2018)

Mach 10.2 Cylinder

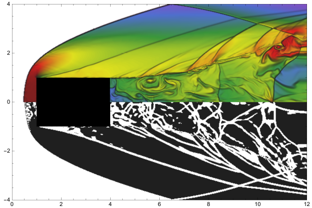

Plot of $log T$ plus simulated Schlieren (top) and Hybrid Switch (bottom)

(Kapper '18)

Entropy Formulation:

- Strong Rarefactions often break Fluid Codes (i.e. Negative Pressures/Artificial Heating)
- Low-β Numerical Instabilities in Apollo (Low-T_e)
- Low-Power Lab Experiments are Low-T_e ($\approx$10eV)
- Relevant Regime Numerically Inaccessible (i.e. T_e<20eV)
- Entropy Cons. Helps for Strong Expansions (Ch.8, Kapper PhD, OSU '09)
- Updated Method Enables Extreme Pressure Ratios (Kapper, 2018)
- Apollo $Q \rightarrow$ Electron Entropy Cons. (Sousa, TBD)
- Extending to Hybrid Energy/Entropy Cons. (Kapper, 2018)

Mach 1.5 Underexpanded Jet

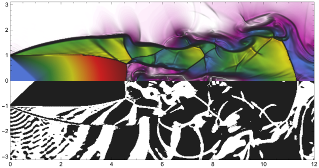

Plot of Mach plus simulated Schlieren (top) and Hybrid Switch (bottom)

(Kapper '18)

Complex Design Space for Pulsed EM:

- Device Geometry: Length/Diameter/Pitch Angle/etc.
- Gas Flow: Mass Flow/Injection/Mixture/Rate/Density/Pre-Ionization
- Electrical: Energy/Coil Shape/Switching Speed/Frequency/Phase/Bias Field

15+ Dimensional Design Space...
Finding 'Good' Designs like a Needle in a Haystack!

Complex Design Space for Pulsed EM:

- Device Geometry: Length/Diameter/Pitch Angle/etc.
- Gas Flow: Mass Flow/Injection/Mixture/Rate/Density/Pre-Ionization
- Electrical: Energy/Coil Shape/Switching Speed/Frequency/Phase/Bias Field

15+ Dimensional Design Space...
Finding ‘Good’ Designs like a Needle in a Haystack!

Potential Solutions:

- Theory: Simplified Analysis Bounding Envelope/Reducing Dimension
- Build and Bust: Fix Physical Constraints and Explore
- Simulation: Requires DNS or Model with Extrapolative Power! (Validated)
- Machine Learning: Finding the Curve beyond Theory (Exp. or Sim.)
- Data Fusion: Accelerating Exp. Knowledge → Models that Extrapolate (Both)

Complex Design Space for Pulsed EM:

- Device Geometry: Length/Diameter/Pitch Angle/etc.
- Gas Flow: Mass Flow/Injection/Mixture/Rate/Density/Pre-Ionization
- Electrical: Energy/Coil Shape/Switching Speed/Frequency/Phase/Bias Field

15+ Dimensional Design Space...
Finding 'Good' Designs like a Needle in a Haystack!

Potential Solutions:

- Theory: Simplified Analysis Bounding Envelope/Reducing Dimension
- Build and Bust: Fix Physical Constraints and Explore
- Simulation: Requires DNS or Model with Extrapolative Power! (Validated)
- Machine Learning: Finding the Curve beyond Theory (Exp. or Sim.)
- Data Fusion: Accelerating Exp. Knowledge $\rightarrow$ Models that Extrapolate (Both)

RMF Characterized by Dimensionless Parameters:

- $\lambda = R/\delta$, where $\delta = (2\eta/\mu_o\omega)^{1/2}$ is the classical skin depth
- $\gamma = \omega_{ce}/\nu_{ei}$, where $\nu_{ei} = \eta(ne^2/m_e)$ is the electron-ion collision frequency

These parameter can be expressed in terms of RMF intensity, frequency and the plasma resistivity:

- $\lambda = R\left(\frac{\mu_o\omega}{2\eta}\right)^{1/2}$ $\qquad$ $\gamma = \frac{1}{e}\left(\frac{B_\omega}{n\eta}\right)$

Theory: Hugrass (Aust. J. Phys. 38, 157 1985)
Semi-Emperical: Milroy (PoP 6, 2771 1999)
(RMF penetration in a fixed ion plasma column)

Question: Does this Relationships hold in MFPM?

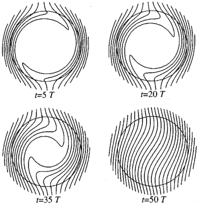

FIG. 1. Evolution of magnetic field lines as the RMF penetrates a plasma column.

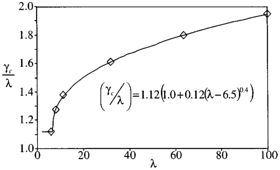

FIG. 4. Critical value of γ vs λ.

Milroy, PoP 6, 2771 (1999)

RMF Characterized by Dimensionless Parameters:

- $\lambda = R/\delta$, where $\delta = (2\eta/\mu_o\omega)^{1/2}$ is the classical skin depth
- $\gamma = \omega_{ce}/\nu_{ei}$, where $\nu_{ei} = \eta(ne^2/m_e)$ is the electron-ion collision frequency

These parameter can be expressed in terms of RMF intensity, frequency and the plasma resistivity:

- $\lambda = R\left(\frac{\mu_o\omega}{2\eta}\right)^{1/2}$ $\qquad \gamma = \frac{1}{e}\left(\frac{B_\omega}{n\eta}\right)$

Theory: Hugrass (Aust. J. Phys. 38, 157 1985)
Semi-Emperical: Milroy (PoP 6, 2771 1999)
(RMF penetration in a fixed ion plasma column)

Question: Does this Relationships hold in MFPM?

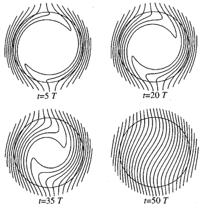

FIG. 1. Evolution of magnetic field lines as the RMF penetrates a plasma column.

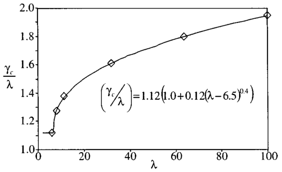

FIG. 4. Critical value of γ vs λ.

Milroy, PoP 6, 2771 (1999)

Machine Learning on MFPM Data:

- Randomly Explored (ω, B_ω, T_e) with MFPM
- Points Plotted w.r.t. (λ, γ) from Theory

MFPM Simulated Dataset

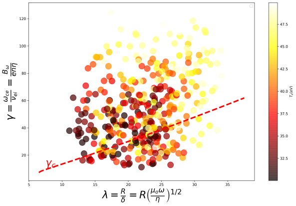

- Density, $n = 1 \times 10^{19} m^{-3}$
- $2\pi \times 10^5 Hz < \omega < 10\pi \times 10^5 Hz$
- $5G < B_\omega < 30G$
- Electron temperature, $30eV < T_e < 50eV$

Machine Learning on MFPM Data:

- Randomly Explored (ω, B_ω, T_e) with MFPM
- Points Plotted w.r.t. (λ, γ) from Theory
- Theory: Necessary but Not Sufficient

Observed B_z-Reversal

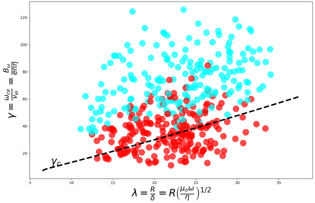

Confusion Matrix

-	Pred No	Pred Yes
Actual No	23	21
Actual Yes	**0**	36

Machine Learning on MFPM Data:

- Randomly Explored (ω, B_ω, T_e) with MFPM
- Points Plotted w.r.t. (λ, γ) from Theory
- Theory: Necessary but Not Sufficient
- Classical Classifiers Explored
- Fewer False Positives & Higher γ_c

Predicted B_z-Reversal Logistic Regression

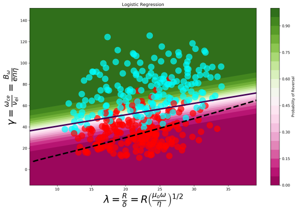

Confusion Matrix

-	Pred No	Pred Yes
Actual No	39	5
Actual Yes	4	32

Machine Learning on MFPM Data:

- Randomly Explored (ω, B_ω, T_e) with MFPM
- Points Plotted w.r.t. (λ, γ) from Theory
- Theory: Necessary but Not Sufficient
- Classical Classifiers Explored
- Fewer False Positives & Higher γ_c
- Balancing Complexity vs. Accuracy?

Predicted B_z-Reversal
K-Nearest Neighbors

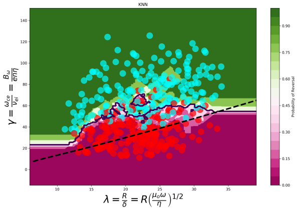

Confusion Matrix

-	Pred No	Pred Yes
Actual No	38	6
Actual Yes	5	31

Learning: RMF Penetration

Machine Learning on MFPM Data:

- Randomly Explored (ω, B_ω, T_e) with MFPM
- Points Plotted w.r.t. (λ, γ) from Theory
- Theory: Necessary but Not Sufficient
- Classical Classifiers Explored
- Fewer False Positives & Higher γ_c
- Balancing Complexity vs. Accuracy?

Predicted B_z-Reversal
Support Vector Machines

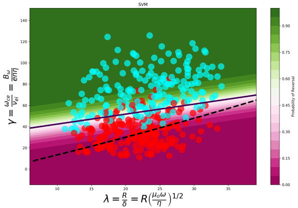

Confusion Matrix

-	Pred No	Pred Yes
Actual No	39	5
Actual Yes	4	32

Machine Learning on MFPM Data:

- Randomly Explored (ω, B_ω, T_e) with MFPM
- Points Plotted w.r.t. (λ, γ) from Theory
- Theory: Necessary but Not Sufficient
- Classical Classifiers Explored
- Fewer False Positives & Higher γ_c
- Balancing Complexity vs. Accuracy?

Predicted B_z-Reversal Random Forest

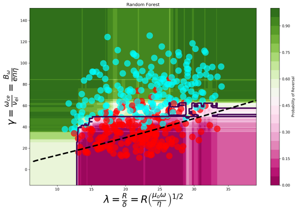

Confusion Matrix

-	Pred No	Pred Yes
Actual No	37	7
Actual Yes	3	33

LEARNING: RMF PENETRATION

Machine Learning on MFPM Data:

- Randomly Explored (ω, B_ω, T_e) with MFPM
- Points Plotted w.r.t. (λ, γ) from Theory
- Theory: Necessary but Not Sufficient
- Classical Classifiers Explored
- Fewer False Positives & Higher γ_c
- Balancing Complexity vs. Accuracy?
- Artificial Neural Network (ANN) with Stochastic Gradient Descent
- Better Classification w/o Extreme Complexity

Predicted B_z-Reversal ANN

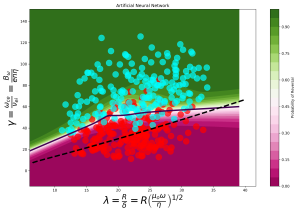

Confusion Matrix

-	Pred No	Pred Yes
Actual No	39	5
Actual Yes	2	34

Machine Learning on MFPM Data:

- Randomly Explored (ω, B_ω, T_e) with MFPM
- Points Plotted w.r.t. (λ, γ) from Theory
- Theory: Necessary but Not Sufficient
- Classical Classifiers Explored
- Fewer False Positives & Higher γ_c
- Balancing Complexity vs. Accuracy?
- Artificial Neural Network (ANN) with Stochastic Gradient Descent
- Better Classification w/o Extreme Complexity

Open Questions:

- Classification Space (λ, γ) Right for MFPM?
- Relevant Dimensions beyond 2D?
- Data Requirements in 3+D Classification?
- Do Experiments Exhibit Similar Trends?

Predicted B_z-Reversal ANN

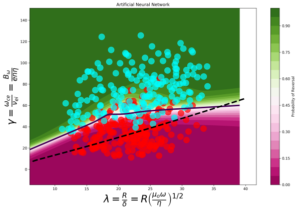

Confusion Matrix

-	Pred No	Pred Yes
Actual No	39	5
Actual Yes	2	34

LEARNING: RMF PENETRATION

Machine Learning on MFPM Data:

- Randomly Explored (ω, B_ω, T_e) with MFPM
- Points Plotted w.r.t. (λ, γ) from Theory
- Theory: Necessary but Not Sufficient
- Classical Classifiers Explored
- Fewer False Positives & Higher γ_c
- Balancing Complexity vs. Accuracy?
- Artificial Neural Network (ANN) with Stochastic Gradient Descent
- Better Classification w/o Extreme Complexity

Open Questions:

- Classification Space (λ, γ) Right for MFPM?
- Relevant Dimensions beyond 2D?
- Data Requirements in 3+D Classification?
- Do Experiments Exhibit Similar Trends?

Predicted B_z-Reversal ANN

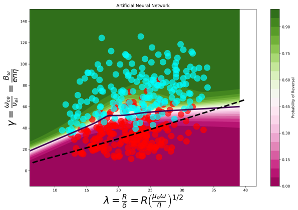

Confusion Matrix

-	Pred No	Pred Yes
Actual No	39	5
Actual Yes	2	34

Curse of Dimensionality:

- Optimization Cost Exponential w/ Dim

Curse of Dimensionality:

- Optimization Cost Exponential w/ Dim
- Not all Dimensions Created Equal!

Active Subspace for Reversal?

Curse of Dimensionality:

- Optimization Cost Exponential w/ Dim
- Not all Dimensions Created Equal!

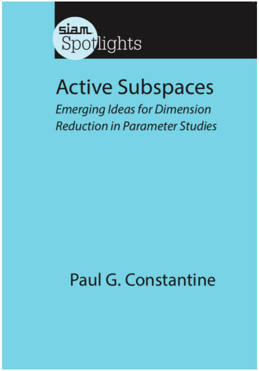

Curse of Dimensionality:

- Optimization Cost Exponential w/ Dim
- Not all Dimensions Created Equal!
- First Step: Identify Dominant Dimensions

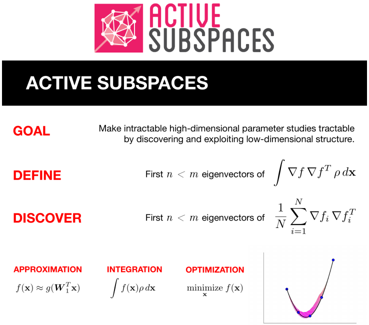

http://activesubspaces.org

Active Subspace for Reversal?

Curse of Dimensionality:

- Optimization Cost Exponential w/ Dim
- Not all Dimensions Created Equal!
- First Step: Identify Dominant Dimensions
- Often Works in Complex Looking Problems (Dominant Low-D Structure is Common)

ACTIVE SUBSPACES

Active subspaces helped us optimize an expensive scramjet model.

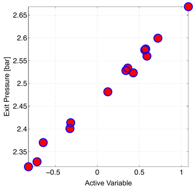

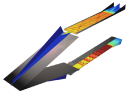

- Multiphysics model of hypersonic scramjet
- 7 input parameters
- No gradients
- Noisy function evaluations
- 2 hours per evaluation

DIMENSION REDUCTION: 7 to 1

http://activesubspaces.org

Curse of Dimensionality:

- Optimization Cost Exponential w/ Dim
- Not all Dimensions Created Equal!
- First Step: Identify Dominant Dimensions
- Often Works in Complex Looking Problems (Dominant Low-D Structure is Common)
- Low-D Structure in Random FRC Data?

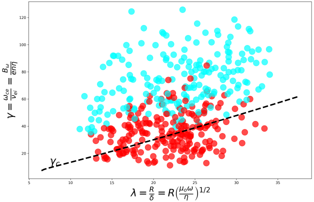

Random Points:

- $2\pi \times 10^5 Hz < \omega < 10\pi \times 10^5 Hz$
- $5G < B_\omega < 30G$
- $30eV < T_e < 50eV$

Curse of Dimensionality:

- Optimization Cost Exponential w/ Dim
- Not all Dimensions Created Equal!
- First Step: Identify Dominant Dimensions
- Often Works in Complex Looking Problems (Dominant Low-D Structure is Common)
- Low-D Structure in Random FRC Data?
- Active Subspace for Min(B_z) in (ω, B_ω, T_e)

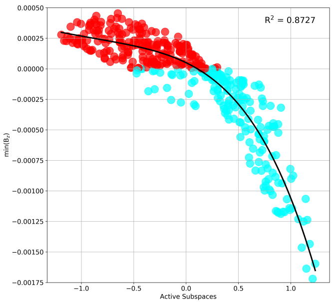

Curse of Dimensionality:

- Optimization Cost Exponential w/ Dim
- Not all Dimensions Created Equal!
- First Step: Identify Dominant Dimensions
- Often Works in Complex Looking Problems (Dominant Low-D Structure is Common)
- Low-D Structure in Random FRC Data?
- Active Subspace for Min(B_z) in (ω, B_ω, T_e)
- Needs Experimental Validation
  - Result Model Artifact?
  - Exp. has Many More Dimensions

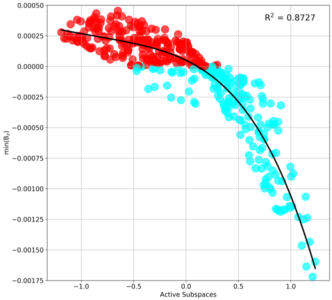

Curse of Dimensionality:

- Optimization Cost Exponential w/ Dim
- Not all Dimensions Created Equal!
- First Step: Identify Dominant Dimensions
- Often Works in Complex Looking Problems (Dominant Low-D Structure is Common)
- Low-D Structure in Random FRC Data?
- Active Subspace for Min(B_z) in (ω, B_ω, T_e)
- Needs Experimental Validation
  - Result Model Artifact?
  - Exp. has Many More Dimensions

EP Exp Produce Data Faster than Simulation

Active Subspaces in the Experimental Loop?

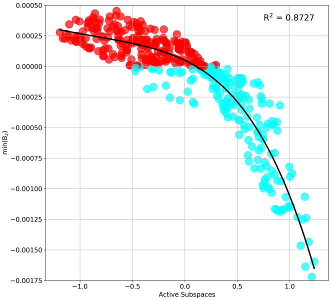

AFRL Pulsed EP Progress:

- Enhanced Models
  - Viscous Multi-Fluid
  - Hybrid Entropy/Energy Conservation
- Improved Understanding
  - Classifiers & Machine Learning
  - Reduced Dimensionality

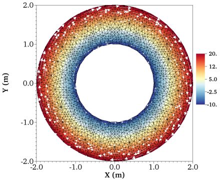

AFRL Pulsed EP Progress:

- Enhanced Models
  - Viscous Multi-Fluid
  - Hybrid Entropy/Energy Conservation
- Improved Understanding
  - Classifiers & Machine Learning
  - Reduced Dimensionality

Near Term Goals:

- Integrate Models
  - Porting DG MFPM to TURF
  - Verify Braginskii Implementation
  - Circuit BCs
  - Radiation Losses
- Re-Engage with Experimental Community

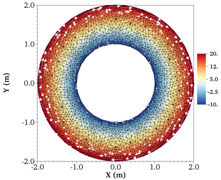

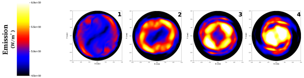

Section: Conclusion and Future Work

AFRL Pulsed EP Progress:

- Enhanced Models
  - Viscous Multi-Fluid
  - Hybrid Entropy/Energy Conservation
- Improved Understanding
  - Classifiers & Machine Learning
  - Reduced Dimensionality

Near Term Goals:

- Integrate Models
  - Porting DG MFPM to TURF
  - Verify Braginskii Implementation
  - Circuit BCs
  - Radiation Losses
- Re-Engage with Experimental Community

Long Term Goals:

- Cross-Verify MFPM/Kinetic Assumptions
- Quantify Extrapolative Model Power
- Optimize Design of Pulsed EP in High-D
- Actively Control Pulsed EP Systems

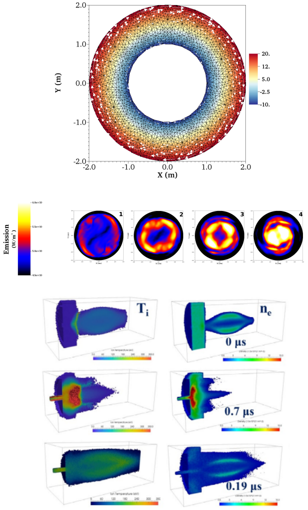

HYPERS Simulation Results for MSX
Omelchenko, *Phys Rev E.* **92**, 023105, 2015

Acknowledgement

Thank You

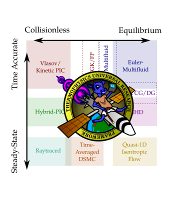

→

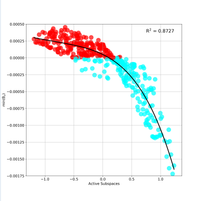

→

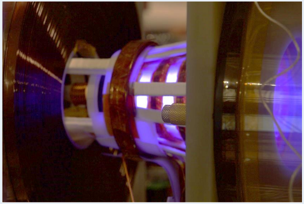

Work Supported through AFOSR Task 17RQCOR465 (PO: Birkan)

Questions?

The Braginskii equations:

- Implementation of Parabolic Flux: $\mathbf{\Pi}_\alpha$, and $\mathbf{q}_\alpha$ (Viscosity & Heat Flux)
- The viscosity begins with the classic Newtonian tensor (1).

$$\overleftrightarrow{\mathbf{W}} = \nabla\mathbf{u} + \nabla\mathbf{u}^T - \left(\frac{2}{3}\nabla\cdot\mathbf{u}\right)\overleftrightarrow{\mathbf{I}} \tag{1}$$

- $\overleftrightarrow{\mathbf{W}}$ is rotated into the magnetic field coordinate frame.
- $\overleftrightarrow{\mathbf{W}}_r$ is then decomposed into parallel, perpendicular, and gyroviscous $\mathscr{W}_i$
- Each of $\mathscr{W}_i$ components is multiplied by a scalar η_i.

Finally,

$$\mathbf{\Pi}_\alpha = rot_{lab}\left(\sum_{i=0}^{N=4}\eta_i\mathscr{W}_i\right) \tag{2}$$